Available online at www.sciencedirect.com
SCIENCE DIRECT®
Journal of Magnetic Resonance 163 (2003) 133–138
JMR Journal of Magnetic Resonance
www.elsevier.com/locate/jmr

Analytical description of GMAX-induced magnetization

João Teles* and Alberto Tannús

Departamento de Física e Informática (FFI - IFSC), Universidade de São Paulo São Carlos, SP 13560-970, Brazil

Received 10 December 2002; revised 25 March 2003

Abstract

The Gradient-Modulated Adiabatic Excitation (GMAX) method is characterized by the use of adiabatic pulses with main applications on volume localization in spectroscopy and slice selection in MRI. Its use derives from the interesting nodal point magnetization profile induced throughout the sample. Nevertheless, the interpretation on such behavior for the magnetization has been of qualitative purpose only, using the adiabatic condition as a starting point. Here, we present discrete spatial analytic solutions, starting from the solution in terms of the hypergeometric functions for sech and tanh pulses. From these discrete solutions, it is possible to infer analytically the characteristic behavior of transverse magnetization, on the purpose to obtain greater control of the magnetization from parameters of the sequence that carry physical interpretation.
© 2003 Elsevier Science (USA). All rights reserved.

Keywords: Solution of Bloch equations; Adiabatic excitation; Gradient-modulated pulses; Phase-modulated pulses; Volume localization

1. Introduction

Slice selection and volume localization are matters of extensive study since the early days of MRI and MRS. They are both examples of the use of static magnetic field gradients to produce a dispersion in the magnetization spectral density. Then, with the use of convenient RF pulses a spatially well-defined magnetization profile is obtained. This picture is somewhat different when non-static magnetic field gradients are applied, and even more curious when the RF pulses are adiabatic.

The behavior of adiabatic pulses, as well as their use in experiments where RF amplitude non-homogeneity is present has been thoroughly discussed in the literature [1–4]. Amongst the sequences that use such pulses, we find GMAX (Gradient-Modulated Adiabatic Excitation) [5,6] as a sequence that presents great advantages in plane selection and volume localization of the sample. It consists basically of the conjoined use of the same modulation function $f(t)$ for the RF frequency, $\omega(t)$, and for the frequency associated to the selection gradient, $\omega_G(x,t) = \gamma B_G(x,t)$,

$$\begin{aligned} \omega(t) &= -\omega_0 - pf(t), \\ \omega_G(x,t) &= qxf(t), \end{aligned} \tag{1}$$

in which p and q are their respective amplitudes, x is the direction of the gradient, and $\omega_0 = \gamma B_0$.

Therefore, in the reference frame rotating with $\omega(t)$, we have for the frequency offset along the z-direction:

$$\Omega(x,t) = [\omega_0 + \omega_G(x,t)] + \omega(t) = f(t)(qx - p). \tag{2}$$

From Eq. (2) we see that Ω has a linear dependence in space, in the x-direction. So, if we use for $f(t)$, and for the transverse field component $B_1(t)$ (RF amplitude), functions that satisfy the adiabaticity criterion and the boundary conditions in $t = -\infty$ and $t = 0$ (see Fig. 1), we will find the transverse magnetization in the x-direction, in $t = 0$, according to Fig. 2a. This is a very interesting magnetization profile, since controlling the amplitude q of $\omega_G(x,t)$ and p of $\omega(t)$ we can choose the inversion point or *spatial node* $x_i = p/q$. Therefore, if we displace x_i of any amount Δx and flip the signal of p or q, the magnetization will result according to Fig. 2b. Adding the two images, we have Fig. 2c, which results in the selection of a slice of the sample. The representation depicted above illustrates the use of the adiabatic half passage, hereafter called GMAX method, as a building block of a slice selection scheme, also called GMAX sequence by their idealizers. This sequence was chosen

* Corresponding author. Fax: +16-273-9876.
E-mail address: jteles@if.sc.usp.br (J. Teles).

1090-7807/03/$ - see front matter © 2003 Elsevier Science (USA). All rights reserved.
doi:10.1016/S1090-7807(03)00127-7

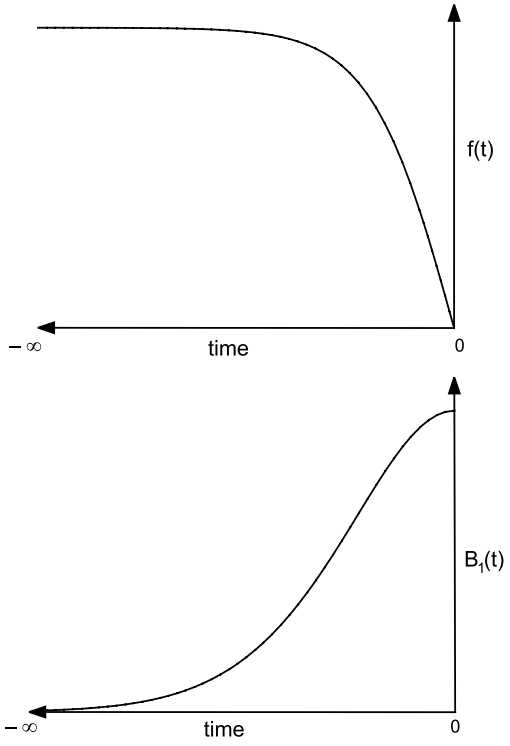

Fig. 1. Initial and final conditions that must be satisfied by the longitudinal and transverse magnetic field components, on top and below, respectively. The pulse must be adiabatic.

for historical reasons to illustrate this work since it was the first proposed use for the GMAX method, although not widely held due to the need of multiple excitations. Adiabatic excitation of any arbitrary nutation angle can be achieved in a single scan using the BISS-8 [7] methodology, also based on the same building blocks of the GMAX method, which therefore could benefit from the use of the results obtained in this work.

Although it is easy to understand how the transverse magnetization is induced along x, it may not be so clear how it behaves at the node in x_i. At this position the longitudinal component of the field is canceled and no longitudinal modulation is present. As a consequence a doubt arises if the magnetization follows or not the adiabatic behavior at this special node. The node x_i has however a simpler description since at this point, in the RF rotating frame, the effective field has only the transverse component along $x : \vec{B}(x_i,t) = B_1(t)\hat{i}$. For a constant direction field, it is known that the magnetization will evolve while keeping a constant angle with the field direction. This can be easily verified by examining the Bloch equation without relaxation as in below.

$$\frac{\mathrm{d}}{\mathrm{d}t}\left[\hat{i}\cdot\vec{M}(x_i,t)\right] = \hat{i}\cdot\frac{\mathrm{d}\vec{M}(x_i,t)}{\mathrm{d}t} = \hat{i}\cdot\left[\vec{M}(x_i,t)\times\gamma B_1(t)\hat{i}\right] = 0. \quad (3)$$

So, the magnetization at x_i will be restricted to the yz-plane contributing with a null value for the x-component. The conclusion is that the behavior at the node satisfies the most common definition of adiabaticity, since that the constant angle between the magnetization and the field in the RF frame is what characterizes this behavior [1]. It lacks however, completion as a

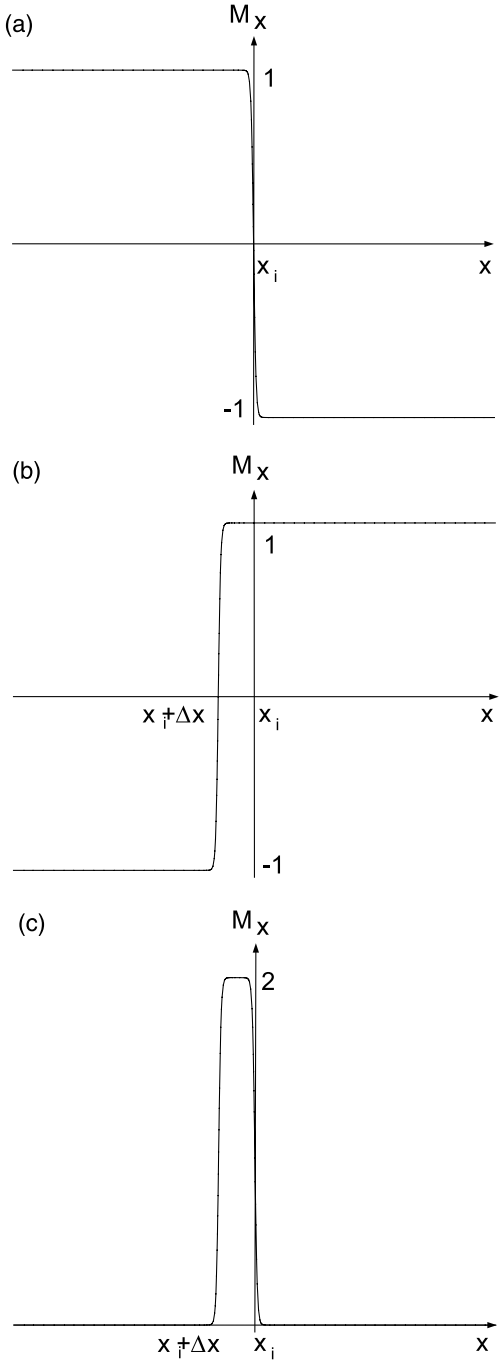

Fig. 2. (a) The magnetization induced along the x-direction with the GMAX methodology, where x_i is the nodal point. (b) The magnetization of the same sample, after parameter changes. Notice the displacement of the nodal point and the inversion of the transverse magnetization sign. (c) The sum of the two magnetizations results in the slice selection of the sample.

definition of adiabaticity in its broadest sense given that this concept is dependent on a comparison between rates of change of the direction of the effective field and the inverse of the relaxation parameters [1]. Another important observation is that the GMAX method is also B_1 insensitive at the node, since a null value for the magnetization component along the effective field in the RF frame is expected for any B_1 amplitude.

The procedure discussed above takes in account a qualitative description based on the assumption that the adiabatic condition is thoroughly satisfied. In fact the expected magnetization of Fig. 2 is observed experimentally as shown by Johnson et al. [5], using NOM [8] optimized adiabatic pulses. Nevertheless, it is important to have some sort of analytical description, which could give details of the magnetization profile. In the following section, we describe the system dynamics using the spinor formalism, which, along with the use of sech and tanh pulses, results in the hypergeometric function. This description is similar to that followed by Hioe [9] and Tannús and Garwood [10], in which the hypergeometric function gives the exact solution for the magnetization. We noticed, however, that at certain discrete positions in space, the hypergeometric function reduces to polynomials. These could be used as a simpler way to describe the magnetization behavior for any point in time, for the specific positions along x.

2. Theoretical development

Previous works [11,12] have demonstrated the efficiency of describing the magnetization in terms of spinors. Firstly, we will describe the magnetization as function of the spin system at a reference frame where the z component of the field vanishes. This choice will show itself a convenient way to obtain the z magnetization component. As this z component is the same in any reference frame where the z-axis coincide, we will change to the frame rotating with the RF frequency $\omega(t)$ and there obtain using the Bloch equations the two other components, M_y and M_x, as a function of the previously obtained M_z.

Given the eigenvectors of the z projection of the angular momentum operator for a particle of spin 1/2, $|\Psi_+\rangle$, and $|\Psi_-\rangle$, we then write the generic state of the state vector as a function of these components,

$$|\Psi\rangle = u|\Psi_+\rangle + v|\Psi_-\rangle. \tag{4}$$

Considering that the spins are isolated (no relaxation effects), the system dynamics will be described by the Schrödinger equation with the Zeeman Hamiltonian:

$$\mathrm{i}\hbar\frac{\partial}{\partial t}\vec{\Psi} = -\vec{\mu}\cdot\vec{B}_{\mathrm{tot}}\vec{\Psi}, \tag{5}$$

where $\vec{\Psi} = \begin{bmatrix} u \\ v \end{bmatrix}$ and $\vec{\mu} = \gamma\vec{S}$. $\vec{S}$ is the spin angular momentum written in terms of the Pauli matrix base,

$$\vec{S} = \frac{\hbar}{2}\left\{\begin{bmatrix} 0 & 1 \\ 1 & 0 \end{bmatrix}\hat{i} + \begin{bmatrix} 0 & -i \\ i & 0 \end{bmatrix}\hat{j} + \begin{bmatrix} 1 & 0 \\ 0 & -1 \end{bmatrix}\hat{k}\right\}.$$

The total magnetic field, in the laboratory reference frame, can be written as a function of the longitudinal $B_z(t)$ and transverse $B_1(t)$ amplitudes:

$$\vec{B}_{\mathrm{tot}}(t) = B_1(t)\left[\hat{i}\cos\Phi(t) + \hat{j}\sin\Phi(t)\right] + B_z(t)\hat{k}. \tag{6}$$

Now we rewrite Eq. (5) in the rotating frame with frequency $-\gamma B_z(t)$. To accomplish this it is sufficient to do the following transformation in the state vector:

$$|\Psi'\rangle = \mathrm{e}^{(\mathrm{i}/\hbar)\theta(t)S_z}|\Psi\rangle, \tag{7}$$

where S_z is the third component of the Pauli matrix and $\theta(t)$ is the angle of rotation, which we have chosen to be $\theta(t) = -\gamma\int B_z(t)\,\mathrm{d}t$. With this transformation we have the new state vector components, U and V, related with the old ones:

$$\begin{aligned} U &= \mathrm{e}^{-(\mathrm{i}/2)\gamma\int B_z(t)\,\mathrm{d}t}u, \\ V &= \mathrm{e}^{(\mathrm{i}/2)\gamma\int B_z(t)\,\mathrm{d}t}v. \end{aligned} \tag{8}$$

Substituting Eq. (8) into Eq. (5) we have the following coupled first-order differential equation system:

$$\begin{bmatrix} \dot{U} \\ \dot{V} \end{bmatrix} = \frac{\mathrm{i}}{2}\gamma B_1(t)\begin{bmatrix} 0 & \mathrm{e}^{-\mathrm{i}\int\Omega\,\mathrm{d}t} \\ \mathrm{e}^{\mathrm{i}\int\Omega\,\mathrm{d}t} & 0 \end{bmatrix}\cdot\begin{bmatrix} U \\ V \end{bmatrix}, \tag{9}$$

where $\Omega(x,t) = \gamma B_z(x,t) + \omega(t)$ and $\omega(t) = \dot{\Phi}(t)$. Now this system can be rewritten as a single second-order differential equation for U:

$$\ddot{U} + \left(\mathrm{i}\Omega(x,t) - \frac{\dot{B}_1(t)}{B_1(t)}\right)\dot{U} + \left(\frac{\gamma B_1(t)}{2}\right)^2 U(t) = 0. \tag{10}$$

We expand it further by replacing the functions $\Omega(x,t)$ and $B_1(t)$ for the adiabatic pulses sech and tanh.

$$\begin{aligned} \gamma B_1(t) &= \frac{\alpha}{\pi\tau}\mathrm{sech}\left(\frac{t}{\tau}\right), \\ \Omega(x,t) &= \frac{\beta(x)}{\pi\tau}\tanh\left(\frac{t}{\tau}\right). \end{aligned} \tag{11}$$

It should be noticed that a frequency offset could be added to $\Omega(x,t)$ in the equation above as followed by Hioe [9], giving solution based on elementary functions for a full passage. This procedure was not adopted here because the resultant hypergeometric solution for a half passage could not be reduced to a simple form. Notice that the spatial factor of Eq. (2) is represented by the parameter $\beta(x)$ in Eqs. (11), which is linear in x. Therefore this parameter will be used for now on regarding results that depend on the position.

The functions (11), along with the following variable transformation of t, $z = (1/2)[1 + \tanh(t/\tau)]$ turn Eq. (10) into the hypergeometric equation given below,

$$z(1-z)\frac{\partial^2}{\partial z^2}U + [c - (a+b+1)z]\frac{\partial}{\partial z}U - abU = 0, \quad (12)$$

in which

$$a = \frac{1}{2\pi}[\phi(x) + \mathrm{i}\beta(x)],$$

$$b = \frac{1}{2\pi}[-\phi(x) + \mathrm{i}\beta(x)] \quad \text{and} \quad \phi(x) = \sqrt{\alpha^2 - \beta(x)^2},$$

$$c = \frac{1}{2}\left[1 + \mathrm{i}\frac{\beta(x)}{\pi}\right]. \quad (13)$$

For the range $0 < z < 1$, which corresponds to $-\infty < t < \infty$, the solution in terms of the hypergeometric function is

$$U = a_1 F(a, b, c; z) + a_2 z^{1-c} F(a - c + 1, b - c + 1, 2 - c; z). \quad (14)$$

At this point, Hioe [9] solved Eq. (12), forcing the initial condition $M_z(z = 0) = -1$. For magnetic resonance systems, the condition $M_z(z = 0) = 1$ is more convenient, from which we end up with the following values for the coefficients: $a_1 = \mathrm{e}^{\mathrm{i}\xi}$ and $a_2 = 0$, where ξ is a constant phase which will not affect the final value of the magnetization, and will therefore be ignored. Thus,

$$U = F(a, b, c; z). \quad (15)$$

As stated in Section 1, our objective is to find solutions for the magnetization, which can be expressed by elementary functions. Therefore it is possible to prove that if we set the following values for ϕ in Eq. (13),

$$\phi = (2n-1)\pi, \quad n = 1, 2, \ldots \quad (16)$$

the series representation of Eq. (15) is truncated in a $(n-1)$th degree polynomial in z [13],

$$U = (1-z)^{c^*} \sum_{j=0}^{n-1} \frac{(1-n)_j (n)_j}{(c)_j j!} z^j, \quad (17)$$

where $(n)_j \equiv \Gamma(n+j)/\Gamma(n)$ is the Pochhammer symbol.

For the first values of n, Eq. (17) will yield less complex analytical solutions if compared with the generalized case of Eq. (15). Let us see then how to obtain the magnetization as a function of U.

The macroscopic magnetization will be proportional to the average value of the spin angular momentum, as follows:

$$M_x \propto \overline{S_x} = \langle \Psi | S_x | \Psi \rangle = uv^* + u^* v,$$

$$M_y \propto \overline{S_y} = \langle \Psi | S_y | \Psi \rangle = \mathrm{i}(uv^* - u^* v), \quad (18)$$

$$M_z \propto \overline{S_z} = \langle \Psi | S_z | \Psi \rangle = |u|^2 - |v|^2.$$

The very last of the equations above, along with the normalization condition $\langle \Psi | \Psi \rangle = |u|^2 + |v|^2 = 1$, give us M_z:

$$M_z = 2|u|^2 - 1 = 2|U|^2 - 1. \quad (19)$$

We are now able to find the M_y and M_x components from the Bloch equations without relaxation (hence reduced to ordinary precessing rotor equations) which are simpler to solve at the reference frame rotating with the RF frequency $\omega(t)$:

$$\dot{M}_x = \Omega(x,t) M_y,$$

$$\dot{M}_y = -\Omega(x,t) M_x + \gamma B_1(t) M_z, \quad (20)$$

$$\dot{M}_z = -\gamma B_1(t) M_y.$$

Replacing Eq. (19) in Eqs. (20), we obtain the other two components M_y and M_x,

$$M_y = -\frac{\dot{M}_z}{\gamma B_1(t)} \quad \text{and} \quad M_x = \frac{\gamma B_1(t) M_z - \dot{M}_y}{\Omega(x,t)}. \quad (21)$$

Therefore, given the value of U, we are able to obtain the final value for the magnetization.

3. Discussion

It is important to note that the restriction imposed to ϕ in Eq. (16) also restricts the values of x to those for which the solutions are similar in form to that of Eq. (17). In fact, we will have a finite number of solutions within the interval $|\beta| \leqslant |\alpha|$. We found that these solutions can be expressed as odd powers of hyperbolic secants with order equal to $2n - 1$. Let us examine how the solutions come out for $n = 1$ and $n = 2$, respectively,

$$M_x\left(\beta = \pm\sqrt{\alpha^2 - \pi^2}, t\right) = \mp\sqrt{1 - \left(\frac{\pi}{\alpha}\right)^2}\,\mathrm{sech}\left(\frac{t}{\tau}\right),$$

$$M_x\left(\beta = \pm\sqrt{\alpha^2 - (3\pi)^2}, t\right) = \mp\left\{\frac{\alpha\sqrt{\alpha^2 - 9\pi^2}}{\alpha^2 - 8\pi^2}\mathrm{sech}\left(\frac{t}{\tau}\right) - \frac{4\pi^2\sqrt{\alpha^2 - 9\pi^2}}{\alpha(\alpha^2 - 8\pi^2)}\mathrm{sech}^3\left(\frac{t}{\tau}\right)\right\}. \quad (22)$$

As we can see, in $t = 0$ the transverse component M_x shows opposite signs at equal distances to $\beta = 0$, which is in accordance to the expected magnetization after qualitative analysis. The curves corresponding to Eq. (22) are depicted in Fig. 3, in which we used $\alpha = 4\pi$ and $\tau = 1$. The plot in Fig. 4 shows a good outline of the results obtained. On top we see the magnetization curves as a function of t, for distinct values of β, which admit solutions given by Eq. (17). Plotted on the bottom we see the magnetization M_x in $t = 0$ for every β using the general form of Eq. (15). The dashed lines indicate the discrete positions for which we obtained solutions. For this case, the values we used for plotting were $\alpha = 10\pi$ and $\tau = 1$.

Yet, it is possible to enhance our analysis by observing the behavior of the magnetization M_z. A neces-

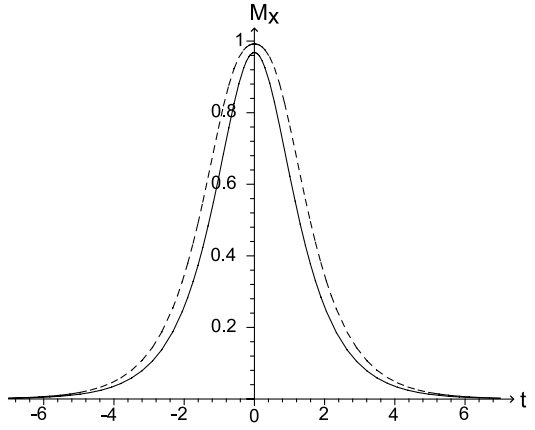

Fig. 3. Corresponding curves for the two first spatial discrete solutions for the x component of magnetization, with pulse parameters $\alpha = 4\pi$ and $\tau = 1$.

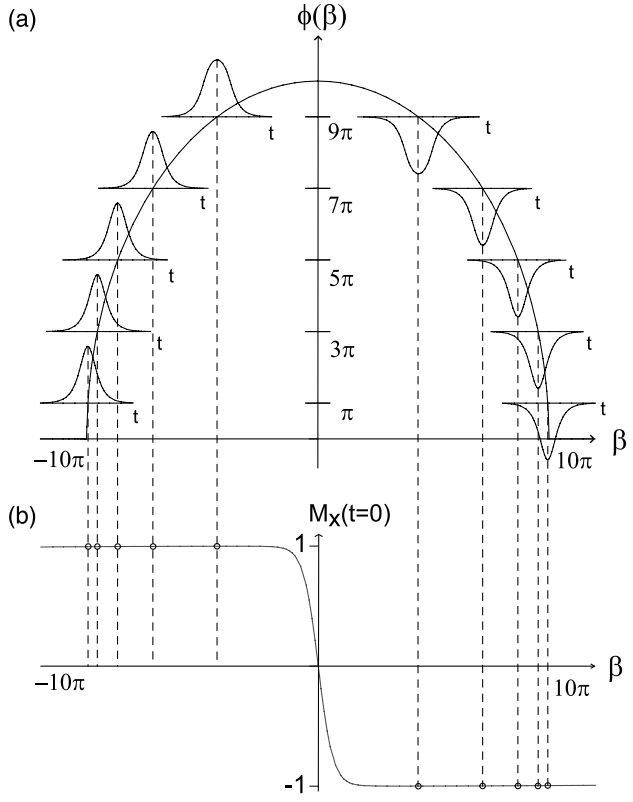

Fig. 4. (a) Transverse magnetization time-profiles, plotted to show the discrete positions where the simpler solutions from Eq. (17) were obtained. (b) Magnetization along x at time zero. This continuous curve was obtained from the general expression Eq. (15). The dots are the points also obtained with the simpler solution.

sary condition for the maximum values of $M_x = \pm 1$ to be reached, in positions excluding the nodal point, is that M_z equals zero in this range. Therefore, one can obtain M_z by substituting Eq. (15) into Eq. (19). Using the following identities [13]:

$$F\left(a, b, \frac{a+b+1}{2}, \frac{1}{2}\right) = \sqrt{\pi}\left\{\Gamma\left(\frac{a+b+1}{2}\right)\Big/\Gamma\left(\frac{a+1}{2}\right)\Gamma\left(\frac{b+1}{2}\right)\right\},$$

$$\Gamma\left(\frac{1}{2}+\mathrm{i}z\right)\Gamma\left(\frac{1}{2}-\mathrm{i}z\right) = \frac{\pi}{\cosh(\pi z)}, \tag{23}$$

we get

$$M_z(t=0) = \cos\left(\frac{\phi}{2}\right)\mathrm{sech}\left(\frac{\beta}{2}\right). \tag{24}$$

Eq. (24) shows that the width of M_z is determined by $\mathrm{sech}(\beta/2)$ in the range that ϕ is real, i.e., $|\beta| \leqslant |\alpha|$. Consequently, the maximum inversion sharpness is also dictated by the $\mathrm{sech}(\beta/2)$. Fig. 5 illustrates this argument. Therefore, following our notation, the width of M_z is only a function of β. However, the β dependence on x has two parameters. This can be seen by identifying in the frequency pulse of Eq. (11) the components of Eq. (2), $\beta = qx - p$ and $f(t) = \tanh(t/\tau)$, which results in the following relation for the widths:

$$\Delta x = \Delta\beta/\pi\tau q. \tag{25}$$

Then, given a specific $\Delta\beta$, the width Δx will be inversely proportional to the pulse width τ and gradient amplitude q. For the range $|\beta| \geqslant |\alpha|$, ϕ turns into pure imaginary and M_z goes to one in the limit that $|\beta| \to \infty$, as

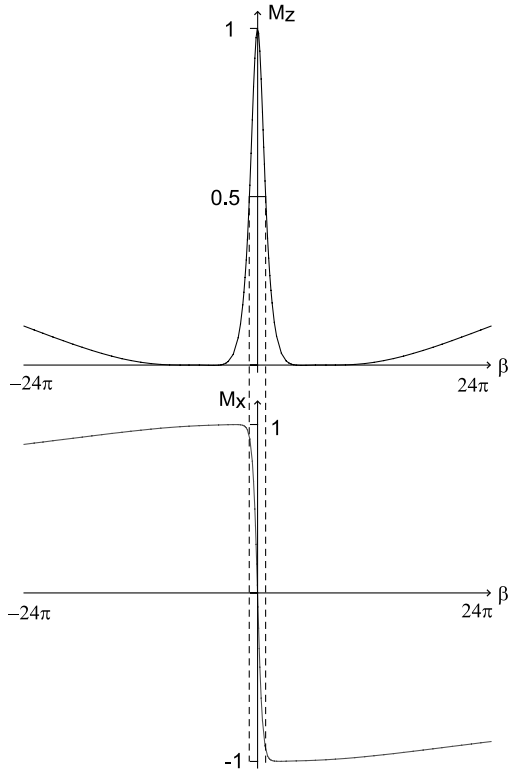

Fig. 5. Relation among z magnetization profile sharpness and x profile inversion sharpness. The best possible sharpness for the M_x inversion profile will be when de y component is zero. In this case the M_x profile will be as steep as the M_z profile is narrow.

shown in Fig. 5. This tendency is not strange since for large β the adiabatic condition is no longer satisfied.

It is interesting to notice that if we set a spatial dependence on the RF amplitude α in such a way that ϕ holds constant, we obtain an exact result such as given by Eq. (17), without any restrictions for x. Therefore, with $\alpha(x) = \sqrt{\phi^2 + \beta(x)^2}$, for $t = 0$ and $\phi = \pi$, we have:

$$M_x(x) = \frac{-\beta(x)}{\sqrt{\pi^2 + \beta(x)^2}}. \tag{26}$$

This magnetization has the same form of the one in Fig. 2a. It is important to notice that such analysis could be made with any other value of ϕ as long as it satisfied Eq. (16), whereas we chose $\phi = \pi$ merely for purpose of simplification.

4. Conclusions

We presented in this work an analytical description for the magnetization of samples exposed to a GMAX methodology. Starting from the quantum description of a non-interacting spin system, we found a solution in terms of the hypergeometric function. Aiming to obtain the clearest understanding of the magnetization behavior, we analyzed the solutions at positions for which the hypergeometric function reduces to polynomials. As a matter of fact we believe that it simplified the description of the magnetization. It was also possible to delineate the maximum inversion sharpness of the x component of magnetization from the behavior of its z component.

Finally we proposed an experiment, where a specific spatial dependence in the RF amplitude modulation that keeps ϕ constant, produces a very simple solution for the desired magnetization inversion profile. This would allow a great deal of control and prediction for the methodology.

Acknowledgment

This work was supported by the Brazilian agency CAPES.

References

[1] C.P. Slichter, Principles of Magnetic Resonance, third ed., Springer, New York, 1990.
[2] A. Tannús, M. Garwood, Improved performance of frequency-swept pulses using offset-independent adiabaticity, J. Magn. Reson. A 120 (1996) 133–137.
[3] A. Tannús, M. Garwood, Adiabatic pulses, NMR Biomed. 10 (1997) 423–434.
[4] R.A. de Graaf, K. Nicolay, Adiabatic rf pulses: applications to in vivo NMR, Concepts Magn. Reson. 9 (4) (1997) 247–268.
[5] A.J. Johnson, M. Garwood, K. Ugurbil, Slice selection with gradient-modulated adiabatic excitation despite the presence of large B_1 inhomogeneities, J. Magn. Reson. 81 (1989) 653–660.
[6] A. Tannús et al., Localized proton spectroscopy with 3D- GMAX, in: 9th Society of Magnetic Resonance in Medicine, August 18–24, New York, NY, 1990.
[7] R.A. de Graaf, K. Nicolay, M. Garwood, Single-shot, B_1-insensitive slice selection with a gradient-modulated adiabatic pulse, BISS-8, Magn. Reson. Med. 35 (1996) 652–657.
[8] K. Ugurbil, M. Garwood, A. Rath, Optimization of modulation functions to improve insensitivity of adiabatic pulses to variations in B_1 magnitude, J. Magn. Reson. 80 (1988) 448–469.
[9] F.T. Hioe, Solution of Bloch equations involving amplitude and frequency modulations, Phys. Rev. A 30 (1984) 2100–2103.
[10] A. Tannús, M. Garwood, Analytical solutions of the Bloch equations for RF pulses which include time-dependent magnetic field gradients, in: 5th Meeting of International Society of Magnetic Resonance, Vancouver, BC, Canada, 1997.
[11] C. Barrat, The application of Spinors to solving the Bloch equations, J. Magn. Reson. 85 (1989) 35–41.
[12] A. Takahashi, T. Peters, Y. Takahashi, The utility and limitations of the spinorized Bloch equations, J. Magn. Reson. 98 (1992) 147–152.
[13] M. Abramowitz, I.A. Stegun, Handbook of Mathematical Functions: with Formulas, Graphs, and Mathematical Tables, Dover, New York, 1964.